Biological and Antioxidant Activities of the Ethanol Extract of Natural Sources and its Nanoparticles from Red tea, Green tea, Roselle, Fenugreek and Ginger

(Received: 08. 03. 2025; Accepted: 26.03.2025)

Emad A. Shalaby, Ahmed Adel Salah El-din, Nermin Elsayed Mohamed, Nadeen Saleh Bahlol and Eman Ahmed Hanafy *

Department of Biochemistry, Faculty of Agriculture, Cairo University, Giza, 12613, Egypt;
* The corresponding author e-mail address: eman.hanafy@cu.edu.eg

ABSTRACT

Nano biotechnology has huge potential in a variety of biological sciences. It involves using particles smaller than 100 nm in size. Due to the disadvantages of chemical nanoparticle synthesis, there is an increasing demand for green nanoparticle synthesis. In particular, AgNPs are essential to nanomedicine and other fields of nanoscience and nanotechnology. While many noble metals have been applied for a variety of uses, AgNPs have received particular attention due to their potential for use in the treatment and diagnostics of cancer. The current research indicates that biosynthesis of green AgNps using five different plant ethanolic extracts (red tea, green tea, roselle, fenugreek, and ginger) is the best approach for producing metal nanoparticles in order to avoid using toxic and high-energy physical and chemical processes. Determination of phenolics, flavonoids, and catechins was performed, and UV–visible spectroscopy, zeta potential, and FTIR were analyzed. In addition, the antioxidant activity against DPPH, ABTS, and $KMnO4$ was evaluated. As well, the cytotoxicity of ginger nanoparticles is tested against HepG2 cell lines. According to the results, ginger AgNp has a significant antioxidant capacity that exceeds that of ascorbic acid and moderate toxicity to HepG2, with an IC50 of 424.62 µg/mL. Green chemistry is important in many areas, including health, where we discovered that plant-based nanoparticles are very antioxidant-rich and have strong antioxidant and anti-cancer properties.

Key words: *Green nanoparticles synthesis, antioxidant, cytotoxicity, plant extracts.*

INTRODUCTION

Nanotechnology is the branch of science that is concerned with studying materials generally sized between 1 and 100 nm. It is a science that acts at the nanoscale and has a vital role in many branches of science, like dentistry, pharmaceuticals, and bio engineering. Solvents and reducing

agents responsible for the reduction of the nanoparticles (NPs) have a great effect on the morphology of incorporated particles like their size, physicochemical properties, and shape, and this morphology impacts on the utilisation of NPs (Jeevanandam et al., 2018).

Physicochemical methods can be used to create NPs. The unique properties of the NPs synthesised by biological methods are preferred over nanomaterials produced by physico–chemical methods (Singh et al. 2015). However, these methods are capital intensive and have many problems, including the use of toxic solvents, the generation of harmful by-products, and the imperfection of the surface structure. Due to the composition uncertainty and lack of predictability, chemical procedures typically consist of multiple chemical species or molecules, which could enhance particle reactivity and toxicity and affect human health and the environment (Li et al., 2011). The future of nanomaterials depends on the use of green chemistry. As opposed to those made via physico-chemical methods, particles made using green synthesis are expected to be far safer, more environmentally friendly, and more widely accepted in nanotechnology. (Hano and Abbasi, 2022).

For the synthesis of metal or metal oxide NPs, green synthesis, a bottom-up approach, substitutes an expensive chemical reducing agent with an extract from a natural product, such as leaves from trees, crops, or fruits. There is huge potential for the creation of NPs in biological beings. Moreover, biogenic reduction of metal precursors to corresponding NPs is eco-friendly, sustainable, free of chemical contamination (Chandran et al., 2006; Huang et al., 2007), less expensive (Mittal et al., 2013) and suitable for mass production (Iravani, 2011). Furthermore, the biological production of NPs allows the recycling of expensive metal salts like gold and silver found in waste streams. These metals have limited resources and have fluctuating prices (Gopinath et al., 2014; Liu et al., 2021). The biological molecules, mostly proteins, enzymes, and sugars, that stabilise NPs easily allow NPs to interact with other biomolecules and thus increase the biological activities by improving the interactions with biomolecules (Yazdanian et al., 2022). The biological formation of NPs permits easy separation of the NPs from the reaction media or up-concentration by centrifugation (Sintubin et al., 2009).

Among the biological entities mentioned above, plants or their extracts seem to be the best agents because they are easily available, suitable for mass production of NPs, and their waste products are eco-friendly (Lee et al., 2011), unlike some microbial extracts. Despite a great deal of research in nanotechnology using physico–chemical approaches, the synthesis of silver (Ag) and gold (Au) NPs is widely exploited using green synthesis. However, only a relatively modest number of studies have attempted to elucidate the biosynthesis and potential applications of other metallic and semiconductor NPs.

This research presents an overview of the biosynthesis of silver NPs from some plant extracts (red tea, green tea, roselle, fenugreek, and ginger) and helps to understand the physico-chemical properties of nanoparticles. In addition, we evaluated their antioxidant activity against DPPH, ABTS, and $KMnO_4$. The cytotoxic effect of ginger against HepG2 carcinoma cells will also be evaluated.

MATERIALS AND METHODS

Chemicals and reagents

Pure ethanol and methanol were purchased from E. Merck Co. (Darmstadt, Germany). Sulfarhodamine, 2, 2 diphenyl-1-picrylhydrazyl (DPPH), 2, 2'- azino-bis ethylbenzthiazoline-6-sulfonic acid (ABTS), 3-(4,5-dimethylthiazol-2-yl)-2,5-diphenyltetrazolium bromide (MTT) Ascorbic acid, Potassium permanganate, Silver nitrate, Sodium hydroxide, Sodium carbonate,

Folin-Denis reagent, Gallic acid, Aluminum chloride, Potassium acetate, vanillin, and Hydrochloric acid were purchased from Sigma-Aldrich (St. Louis, MO, USA).

Cell lines and culture

HepG2 (human liver carcinoma cells) was obtained from the Viscera (Giza, Egypt). Cells were maintained in RPMI-1640 containing 100 µg/mL streptomycin, 100 units/mL penicillin, and 10% heat-inactivated fetal bovine serum in a humidified 5% (v/v) CO_2 atmosphere at 37^{o}C.

Preparation of the plants' leaves ethanolic extract

Healthy seeds of fenugreek (Trigonella foenum-graecum), roots of ginger (Zingiber officinale), flowers of roselle (Hibiscus sabdariffa), leaves of red tea (Camellia spp.), and leaves of green tea (Camellia spp.) were selected, washed several times with tap water and distilled water to remove dust, and the leaves were then air dried to remove any moisture. According to Rossenthaler's (1930) guidelines, each dried leaf was crushed in a mortar before being extracted with 2000 mL of ethanol. The extract was filtered through whatman No. 1. The extracts were then stored for later use and kept in sterile bottles in a refrigerator at 4°C.

Biosynthesis of silver nanoparticles (AgNPs)

A solution of 1 mM $AgNO_3$ (100 mL) was heated with magnetic stirring at 60–70°C for 45 minutes. Then, 10 mL of extract was added dropwise. The solution's transformation from colourless to brown served as confirmation that Ag+ had been reduced to AgO (Khattak et al., 2019). The synthesised AgNPs were collected by centrifugation and adjusted to an alkaline pH (≥ 9) by the addition of NaOH. The pH measurements were made using a calibrated pH metre at 25°C. All samples were measured before and after the addition of NaOH as shown in table (1). For characterization requirements, a brown powder was obtained and carefully collected.

Table 1: The pH values for produced nanoparticles before and after adding NaOH.

Sample	pH before adding NaOH	pH after adding NaOH
Green Tea	5.4±0.028	9.4±0.068
Red Tea	4.8±0.084	9.4±0.053
Roselle	4±0.097	9.4±0.081
Ginger	5.4±0.033	9.5±0.069
Fenugreek	6.7±0.086	10.5±0.077

Values are mean ± SE (n=3).

Determination of reducing agent.

Determination of total phenolic compounds

The colorimetric method of Folin-Denis as described by Swain and Hillis (1959) was employed for the determination of phenolic compounds. Aliquots of 0.1 g of plant extracts were dissolved in 1 mL of deionized water. The solutions were mixed with 2.8 mL of deionized water, 2 mL of sodium carbonate, and 0.1 mL of 50% Folin-Denis reagent. After incubation at room temperature for 30 min, the absorbance of the reaction mixture was measured at 750 nm against a deionized water blank on a Spectrophotometer (jenway 6305 UV/Vis Spectrophotometer). Gallic acid was used as a standard (0–200 mg/L) for the preparation of the standard curve. Plant extract data were expressed in milligram gallic acid equivalents/g dry weight.

Determination of total flavonoids

The flavonoid content of the extract was determined using the aluminum chloride colorimetric method described by Chang et al. (2002). This method is based on measuring the increase of yellow

color at 415 nm, which is relative to flavonoid content. Aliquots of 0.1 g of extract were dissolved in 1 mL of deionized water. This solution was mixed with 1.5 mL of 95% alcohol, 0.1 mL of 10% aluminium chloride, 0.1 mL of 1 M potassium acetate, and 2.8 mL of deionized water. After incubation at room temperature for 40 min, the reaction mixture absorbance was measured at 415 nm against a deionized water blank on a spectrophotometer (Jen Way 6305 UV/Vis spectrophotometer). Quercetin was chosen as a standard. The total flavonoid content of various plant extracts was determined in triplicate and expressed as milligrams of quercetin equivalents per gram. The results was then converted to milligram quercetin equivalents per gram dry weight of plant extracts.

Determination of condensed tannins

Condensed tannins (catechins) of plant leaf extracts were determined using the vanillin assay described by Belyagoubi-benhammou et al. (2014) with some modifications. To 50 µL of each extract, 1500 µL of vanillin/methanol (4%) solution was added and mixed. Then, 750 µL of concentrated HCl was added and allowed to react at room temperature for one hour. The absorbance at 550 nm was measured against a blank. The total concentration of condensed tannins was expressed in micrograms of catechin equivalents per milligram dry matter with reference to the catechin calibration curve.

Characterization of nanoparticles (NPs-Me)

UV–vis spectrophotometric analysis

The color change of the reaction medium was initially monitored by periodic sampling of reaction solutions and Nps formation was confirmed by measuring its UV–VIS absorption. The aliquots of reaction mixture were measured by an UV-visible spectrophotometer in the range of 300–600 nm as described by Khattak et al. (2019).

Fourier Transform Infrared (FTIR) spectroscopy

FTIR analysis was examined for different biosynthesized nanoparticles using a Shimadzu FTIR spectrometer at room temperature within the wavelength range of 400−4000 cm−1 at a resolution of 3 cm−1 in KBr pellets.

Zeta potential. X-ray diffraction (XRD)

X-ray data of all extracted NPs were obtained using a wavelength-dependent CuKα radiation source (wavelength = 1.5418 Å), at 40 kV and 40 mA, a 2θ range of 20-80°, a step size of 0.02°, and a time/step of 0.6 s, on a D8 Advance with DAVINCI design (Bruker, Germany). The DIFFRAC Measurement Centre Version V7.3.0 (32Bit) software was utilized to operate a Si zero-background sample holder, and the Powder Diffraction Files (PDF) of the COD database were used to assign peaks (Crystallography Open Database).

Antioxidant Activities

DPPH radical scavenging activity

The scavenging activity of different plant extracts and nanoparticles biosynthesized were determined by the method of Yen and Chen (1995), where 2.0 mL of 0.16 mM DPPH solution (in methanol) was added to a test tube containing a 1.0 mL aliquot of sample at 100 and 200 µg/mL. The mixture was vortexed for 1 min and kept at room temperature for 30 min in the dark. The absorbance of all the sample solutions and BHT as a synthetic standard were measured at 517 nm. The percentage (%) of scavenging activity was calculated as follows:

Inhibition (%) = [(A control – A sample) / A control] ×100

Where; A control is the absorbance of DPPH while A sample is the absorbance of the sample.

$KMnO_4$ scavenging method

The scavenging activity of different plant extracts and nanoparticles biosynthesized were determined by the method of Gaber et al. (2021), where 2.0 mL of 0.02M $KMnO_4$ solution (in methanol) was added to a test tube containing a 1.0 mL aliquot of sample at 100 and 200 µg/mL. The mixture was vortexed for 1 min and kept at room temperature for 30 min in the dark. The absorbance of all the sample solutions and ascorbic acid as a natural standard were measured at 514 nm. The percentage (%) of scavenging activity was calculated as follows:

Inhibition (%) = [(A control – A sample) / A control] ×100

Where; A control is the absorbance of DPPH while A sample is the absorbance of the sample.

ABTS radical cation scavenging assay

The ABTS assay was based on the ability of different substances to scavenge 2, 2'-azino-bis ethylbenzthiazoline-6-sulfonic acid ($ABTS^{\cdot+}$) radical cation. The radical cation was prepared by mixing 7 mM ABTS stock solution with 2.45 mM potassium persulfate (1/1, v/v) and leaving the mixture for 4–16 hrs until the reaction was completed and the absorbance was stable. The $ABTS^{\cdot+}$ solution was diluted with ethanol until it gave an absorbance of 0.700±0.05 at 734 nm according to Re et al. (1999). The photometric assay was conducted on 0.9 mL of (ABTS.+) and 0.1 mL of different plant extracts and nanoparticles biosynthesized, mixed for 45 s, and the measurements were taken at 734 nm after 1 min. The following equation was used to determine the decrease in absorbance and to calculate the antioxidant activity of the investigated samples:

E= ((Ac-At)/Ac) x 100

Where: At and Ac are the absorbance's of the tested samples and ABTS.+, respectively.

Cytotoxic activity

Cytotoxic activity of ginger nanoparticles was determined by the MTT protocol according to Slater et al. (1963). The 96-well tissue culture plate was inoculated with 1 X 105 cells/mL (100 µl/well) then incubated at 37°C for 24 hours to develop a complete monolayer sheet. Growth medium was decanted from 96 well micro liter plates after a confluent sheet of cells was formed. The cell monolayer was washed twice with wash media.

The tested samples were diluted two-fold in RPMI medium with 2% serum (maintenance medium). One mL of each dilution was tested in different wells, leaving 3 wells as controls, receiving only maintenance medium. The plates were incubated at 37°C and examined. Cells were checked for any physical signs of toxicity, e.g., partial or complete loss of the monolayer, rounding, shrinkage, or cell granulation.

An MTT solution was prepared (5 mg/mL in Phosphate Buffer Solution). Each well received 20µl MTT solution that was shaken at 150 rpm for 5 minutes to thoroughly mix the MTT into the media.

The MTT was allowed to be metabolized at 37ºC with 5% CO_2 for 4 hours. The media was discarded, and the plate was dried on paper towels to remove residue if necessary. The formazan (MTT metabolic product) was dissolved in 200 µl of DMSO. After being shaken for 5 minutes at 150 rpm to thoroughly mix the formazan into the solvent, optical density was read at 560 nm and subtracted background at 620nm. Optical densities should be directly correlated with cell quantities. Doxorubicin (Dox) was evaluated as a standard drug.

Statistical analysis

Analyses of values use the mean, SE, or SD. The statistical computer application "Costat" was used for the statistical analysis. In the statistical study, one-way analysis of variance (ANOVA), the Student-Newman-Keuls test, and the least significant difference (LSD) at P 0.05 were used.

RESULTS AND DISCUSSION

Total phenolic, Flavonoid and catechin content

The total content of phenolic compounds, flavonoids, and catechins was determined at different wavelengths to evaluate their content in plant extracts, and the results are shown in figure (1).

From the obtained results of phenolic compounds in Figure (1), it was observed that the ginger extract has the highest phenolic compounds content, which is 36.8 mg\g followed by green tea by 22.19 mg\g and red tea by 21.33 mg\g. Both roselle and fenugreek extracts have the lowest value of 7.88 mg\g. From these results, it was found that the ginger extract is the richest extract in phenolic compounds. These findings agreed with those of Ghasemzadeh et al. (2010), who reported that the amount of phenolic chemicals in the extract of ginger leaves and stems was comparable. Polyphenolic compounds were found to have antioxidant properties, and it is likely that these chemicals are responsible for the extracts' effectiveness. This action is thought to be owing to their redox characteristics, which aid in the adsorption and neutralisation of free radicals, the quenching of singlet and triplet oxygen, and the decomposition of peroxides. Red tea polyphenols are strong antioxidants that have the ability to scavenge free radicals in the body (Ahmed and Baral, 2011).

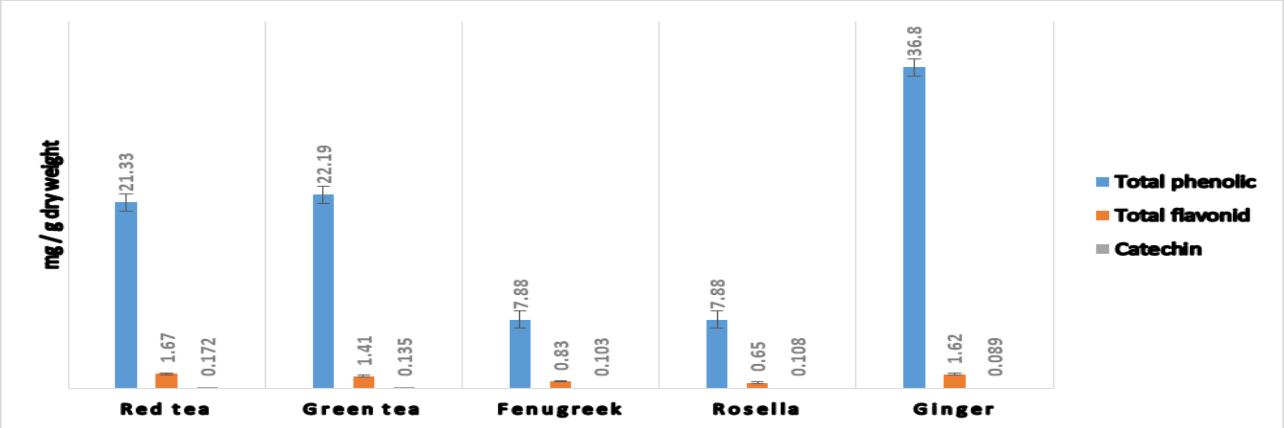

Figure 1. Total phenolic, flavonoid, and catechin content (mg/g) for red tea, green tea, fenugreek, roselle and ginger extracts.

Also, figure (1) showed that the highest flavonoid content was for red tea extract by 1.67 mg\g followed by ginger, which was 1.62 mg\g followed by green tea by 1.41 mg\g, then fenugreek by 0.83 mg\g and lastly, roselle extract by 0.65 mg\g. From these results, we can conclude that red tea extract is the richest in flavonoids. The results were consistent with Dhillon et al. (2021), who stated that red tea is very rich with flavonoids that are primarily responsible for red tea's distinct flavour and color. The difference in the flavonoid content of red tea and green tea may be due to differences in agronomic conditions, processing methods, storage during or after transportation, and the degree of fermentation as stated in Tang et al. (2019).

Finally, as shown in figure (1), red tea extract had the largest amount of catechins, 0.172 mg/g, followed by green tea, 0.135 mg/g, roselle, 0.108 mg/g, fenugreek, 0.103 mg/g, and ginger extract, which had the lowest amount, 0.089 mg/g. According to these findings, red tea has a variety of catechin polymers, similar to green tea. In immature red tea leaves, epigallocatechin-3-gallate is the most active and plentiful catechin polymer, and during fermentation, it transforms into theaflavins and thearubigins.

Between 3% and 5% of the total red tea extract is made up of these catechin-oxidizing polymers, which are essential determinants of red tea quality (Dhillon et al., 2021).

Antioxidant activities

DPPH radical scavenging activity

The DPPH free radical experiment is a spectrophotometric assay used to measure the capacity of antioxidants to decrease an oxidant. DPPH radical scavenging activity of red tea, green tea, roselle, fenugreek, and ginger ethanolic extracts is shown in Table (2). The results indicated that green tea ethanolic extract has the highest DPPH radical scavenger (80.5%), followed by ginger ethanolic extract (80%), followed by the roselle ethanolic extract (78.4%), then the red tea ethanolic extract (67.4%), and the last sample is the fenugreek ethanolic extract (62.8%). These plant extracts contain high amounts of antioxidants as they are rich in phenolics, flavonoids, tannins, sterols, terpenoids, saponins, anthraquinones, alkaloids, and vitamins, so they have high antioxidant activity (Wang et al., 2019).

Table 2. Antioxidant activity (%) of plant ethanol extracts and AgNPs against DPPH assay

Sample	DPPH scavenging activity (%)	
	Ethanol extract	AgNPs
Green tea	80.50±2.59	91.00±2.38
Red tea	67.40±2.21	54.10±3.57
Roselle	78.40±1.92	72.30±3.47
Ginger	80.00±3.09	94.40±1.58
Fenugreek	62.80±3.66	85.60±1.88
Ascorbic Acid	82.6±1.97	

Values are mean ± SE (n=3).

When the DPPH radical scavenging activity of nano red tea, green tea, roselle, fenugreek, and ginger was determined, the nano ginger extract had the highest DPPH radical scavenging activity (94.4%), followed by the nano green tea (91%), followed by the nano fenugreek (85.6%), followed by the nano roselle (72.3%), and the nano red tea had the lowest (54.1%) in comparison to the ascorbic acid standard (82%). Furthermore, Kokila et al. (2022) suggested that the presence of a variety of phytochemicals such as phenolics, flavonoids, and other active substances on the surface as capping agents on the NPs nanoparticles may be the cause of the observed antioxidant activity of AgNPs. Due to their reduced size and stability, AgNPs showed better antioxidant activity than plant extracts in the DPPH radical assay.

$KMnO_4$ scavenging assay

A reduction of the oxidant $KMnO_4$ occurs when antioxidants are present. When it is reduced, a spectrophotometrically measurable colour change takes place.

The results which were obtained in table (3) showed the antioxidant activity in plant ethanolic extracts against $KMnO_4$. The roselle ethanolic extract has the highest antioxidant activity against $KMnO_4$, which recorded 94.7%, followed by the fenugreek ethanolic extract (91.8%), then the red tea ethanolic extract (62.7%), followed by the green tea ethanolic extract (61.4%), and the last one was the ginger ethanolic extract (54%). Furthermore, the results of the AgNPs of examined plants showed that ginger-AgNPs were the richest ones in plant extract (87.2%), followed by fenugreek-AgNPs (69.3%), then red

tea-AgNPs (28.4%), followed by roselle-AgNPs (17.2%), and the green tea-AgNPs, was the lowest one (17%).

Table 3. Antioxidant activity (%) of plant ethanol extracts and AgNPs against $_{KMnO4}$ assay

Sample	$_{KMnO4}$ scavenging activity (%)	
	Ethanol extract	AgNPs
Green tea	61.40±2.01	17.00±0.97
Red tea	62.7±2.69	28.4±0.45
Roselle	94.7±1.37	17.2±0.38
Ginger	54.00±1.25	87.20±0.58
Fenugreek	91.80±1.94	62.7±0.81
Ascorbic Acid	78.95±2.61	

Values are mean ± SE (n=3).

ABTS radical scavenging activity

The provided data in table (4) demonstrated the antioxidant activity of plant ethanolic extracts against the ABTS cation radical. The antioxidant activity of the red tea ethanolic extract was found to be the highest at 68.2%, followed by the fenugreek ethanolic extract at 43.2%, followed by the roselle ethanolic extract at 39.05%, then the green tea ethanolic extract at 37.6%, but ginger ethanolic extract showed the weakest one at 27.35%. These results were compared with ascorbic acid as a natural antioxidant compound, which recorded 86.39% against the ABTS radical.

Table 4. Antioxidant activity (%) of plant ethanol extracts and AgNPs against ABTS

Sample	ABTS scavenging activity (%)	
	Ethanol extract	AgNPs
Green tea	37.60±1.07	52.36±0.72
Red tea	68.20±1.82	78.12±0.93
Roselle	39.05±1.33	43.89±1.08
Ginger	27.35±2.81	40.99±1.07
Fenugreek	43.20±1.98	56.17±1.81
Ascorbic Acid	86.39±1.22	

Values are mean ± SE (n=3).

AgNPs Characterization

UV–vis spectrophotometric assay

Figures 2 and 3 demonstrate an analysis of the wave length of the ethanolic extract and AgNPs of the studied plants, respectively, using UV-vis spectrophotometry.

In Figures 2 and 3, the λ max of plant ethanolic extracts as well as plants' AgNPs were indicated. The results indicated that fenugreek has the highest ehanolic extract and AgNPs λ max at an absorbance of 1.384. Red tea AgNPs λ max was decreased from an absorbance of 1.359 for ethanolic extract to 1.105. The green tea AgNPs λ max was decreased from an absorbance of 1.07 for ethanolic extract to 0.483. Also, roselle AgNPs λ max was decreased from an absorbance of 1.033 for ethanolic extract to 1.05. Finally, ginger AgNPs λ max was decreased from an absorbance of 1.02 for ethanolic extract to 0.286.

The differences in their size, shape, and aggregation status may explain the decrease seen in λ max of AgNPs generated using ethanolic extracts (Tak et al., 2015). Our results agree with those from previous findings by Firoozi et al. (2016) and Ramesh et al. (2018) using different extracts.

3.3.2. Fourier Transform Infrared (FTIR) spectroscopy.

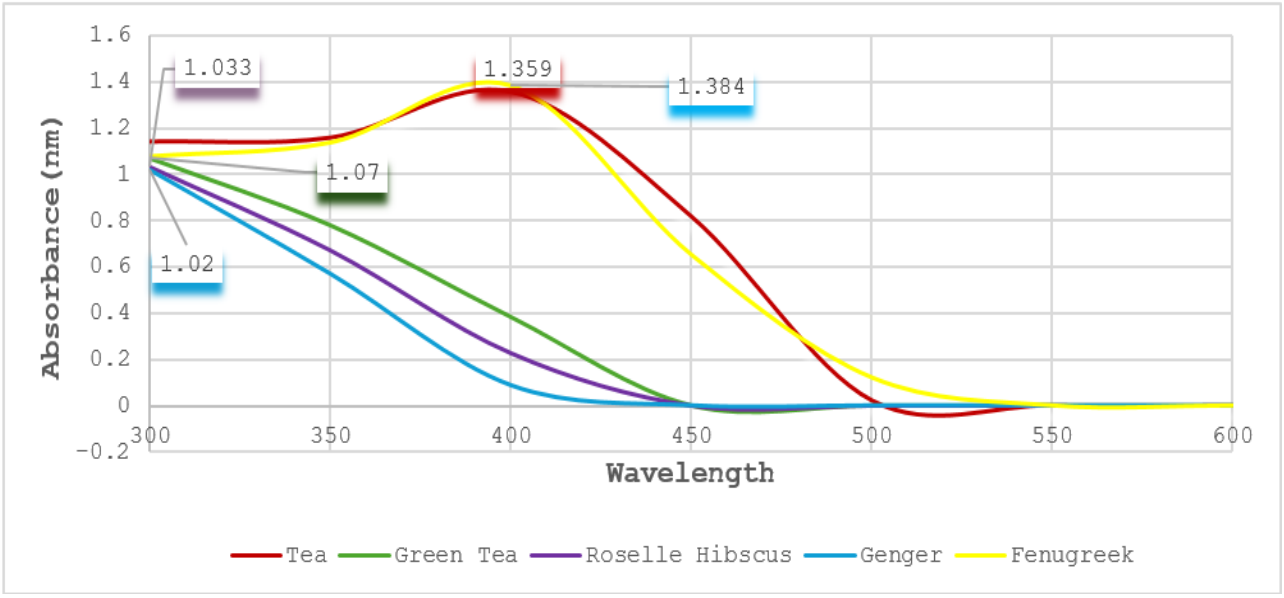

Figure 2. U.V spectrometer for red tea, green tea, fenugreek, roselle and ginger extracts.

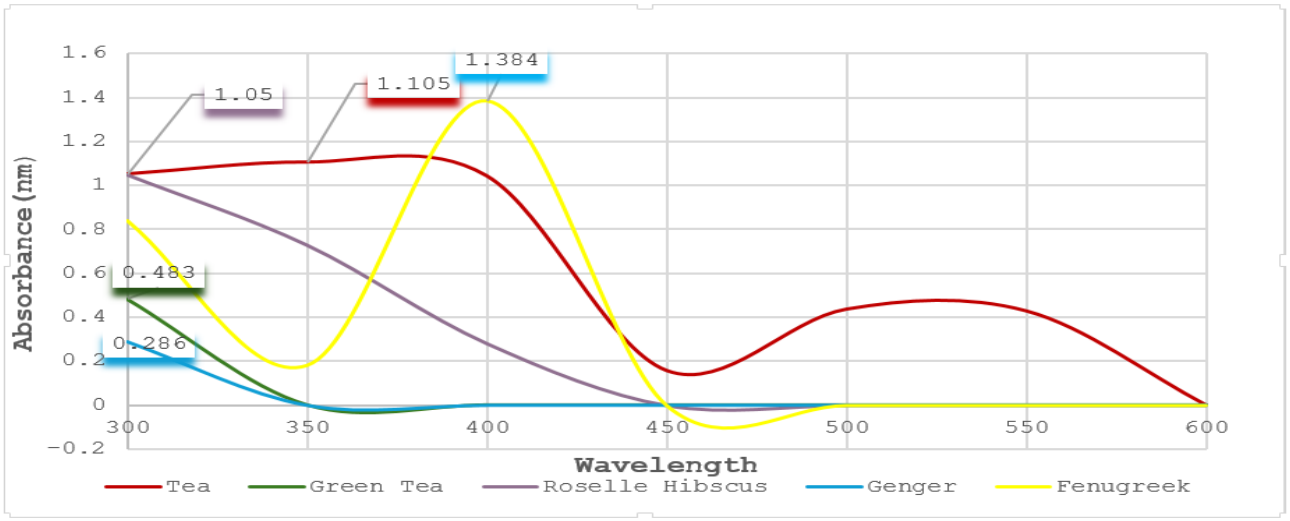

Figure 3. U.V spectrometer for red tea, green tea, fenugreek, roselle and ginger nanoparticles.

Figures (4-8) and table (5) illustrate the FTIR results of various plant ethanolic extracts and their green synthesized AgNPs.

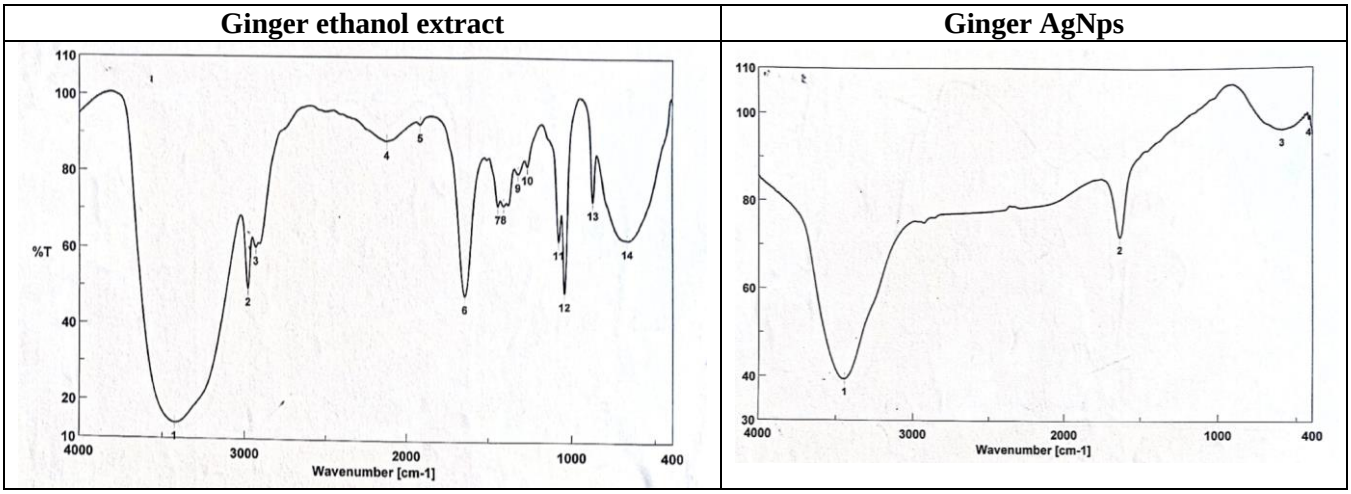

Figure 4. FTIR Spectrum for ginger ethanol extract and ginger AgNPs

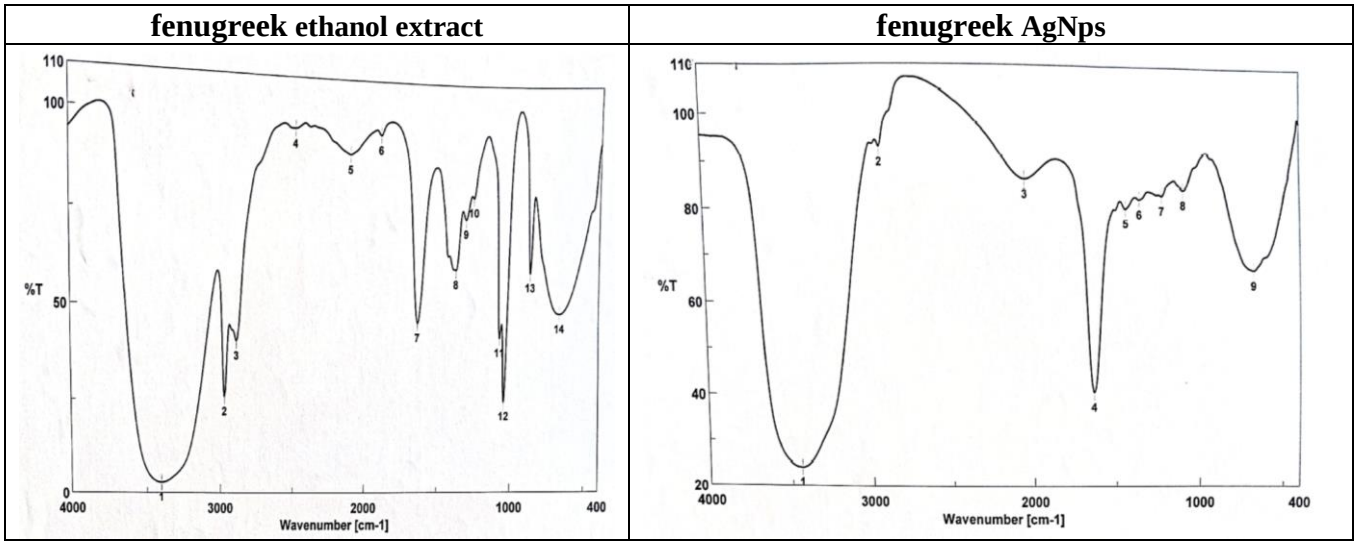

Figure 5. FTIR Spectrum for fenugreek ethanol extract and fenugreek AgNPs

Red tea ethanol extract	**Red tea AgNps**
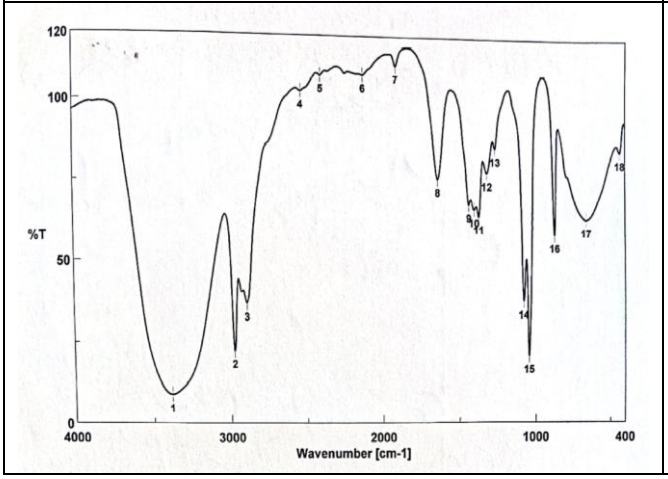	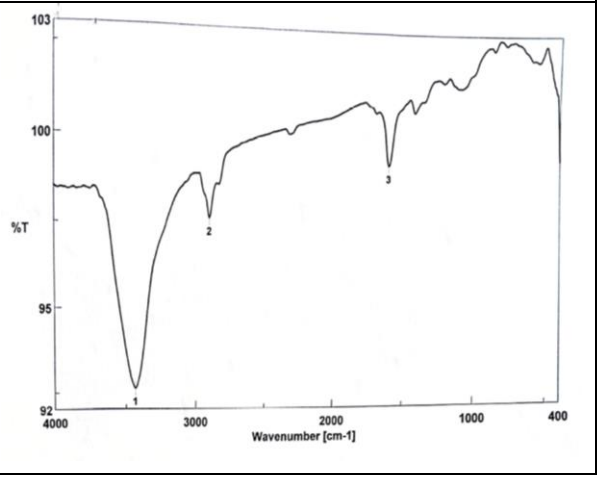

Figure 6. FTIR Spectrum for red tea ethanol extract and red tea AgNPs

Roselle ethanol extract	**Roselle AgNps**
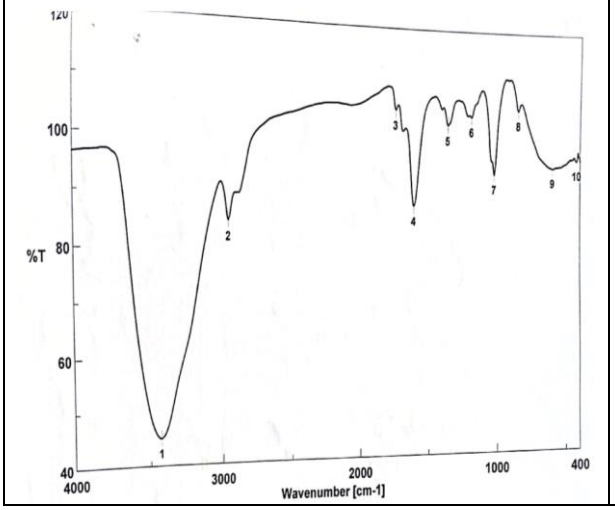	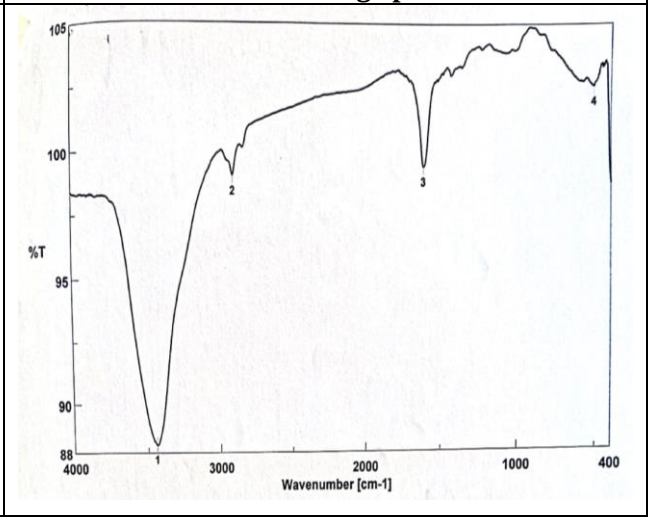

Figure 7. FTIR Spectrum for roselle ethanol extract and roselle AgNPs

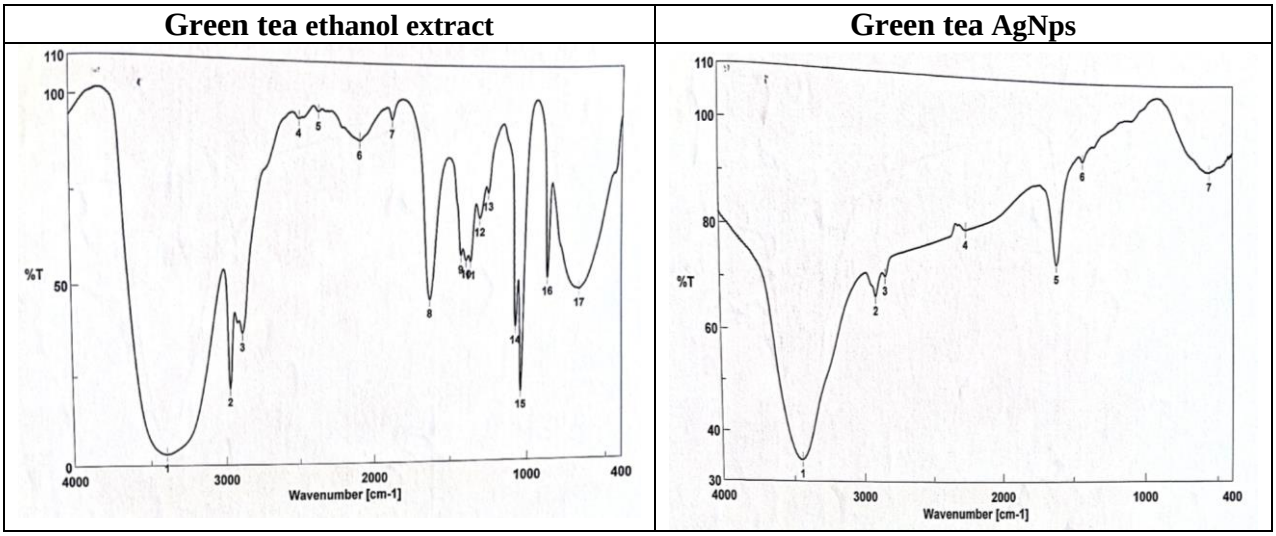

Figure 8. FTIR Spectrum for green tea ethanol extract and green tea AgNPs

Table 5: Active groups of different plant extract identified using FTIR.

Active group	Ginger		Fenugreek		Red Tea		Roselle		Green Tea	
	Native	**Nano**	**Native**	**Nano**	**Native**	**Nano**	**Native**	**Nano**	**Native**	**Nano**
O-H	3425.9	3444.2	3402.8	3441.3	3381.5	3434.6	3429.8	3441.3	3397.9	344.2
C-H	2976.6	ND	2976.6	2926.4	2975.6	2923.5	2979.5	2923.5	2976.6	2924.5
C-H	2928.4	ND	2897.5	ND	2893.6	ND	1637.3	1637.3	2896.5	2857.9
N=N=N C≡C	2125.2	ND	2130.9	2057.6	1652.7	1633.4	1401	ND	1648.8	1638.2
C=O	1644.9	1639.2	1647.8	1457.9	1449.2	ND	-----	-----	1449.2	1461.7
C-O/C-C/COO	1450.2	ND	-----	-----	1414.5	ND	-----	-----	1415.5	ND
	1415.3	ND	-----	-----	1383.7	ND	-----	----	1385.6	ND
Amide	1329.7	ND	1392.3	1375.9	1329.7	ND	-----	-----	1328.7	ND
Amide	1274.7	ND	1327.7	1242.9	1275.7	ND	1226.5	ND	1276.6	ND
C-O	1084.7	ND	1276.6	1114.6	1086.7	ND	1048.1	ND	1086.7	ND
C-O	1047.2	ND	1083.8	ND	1048.1	ND	874.5	ND	1047.1	ND
C-H	878.4	594.9	1048.1	ND	-----	-----	610.3	513.9	879.4	ND
C-O	671.1	423.3	671.1	686.53	665.3	ND	428.1	ND	672.1	563.11

ND: Not detected.

The results of ginger ethanolic extract an its AgNps in figure (4) indicate that the instinct absorption bands in AgNPS at 3444.2 cm^{-1} and ginger ethanolic extract at 3425.9 cm^{-1} appear in the presence of a free OH group. The ethanolic extract exhibits the absorption bands at 1644.9 cm^{-1} and 1639.2 cm^{-1} in AgNPs while the C=O group is present. The exanolic extract exhibits three absorption bands at 2976.6, 2928.4, and 878.4 cm^{-1} in the presence of the C-H group, whereas the AgNPs only exhibit one band at 594.9 cm^{-1}. The ethanolic extracts exhibit the absorption bands at 1084.7, 1047.2, and 671.1 cm^{-1} in the presence of the C-O group, whereas the AgNPs exhibit them only once at 423.3 cm^{-1}. The absorption bands were only present in the ethanolic extracts and not in the AgNps in the presence of C-H, N=N=N, C-C, COO, and amide groups.

As shown in figure (5), all of the fenugreek extract's absorption bands are detectable in the ethanolic extract and AgNPs when all of the active groups are present, but when the C-H group is present, only three of the bands at 2976.6, 2897.5, and 1048.1 cm-1 are visible and only once at 2926.4 cm^{-1}. The ethanolic extract exhibits three absorption bands at 1276.6, 1083.8, and 671.1 cm^{-1} in the presence of the C-O group, but the AgNPs only exhibit one band at 686.53 cm^{-1}.

For red tea extract, as shown in figure (6), the absorption bands only appear in the ethanolic extract in the presence of all active groups, with the exception of the O-H, C-H, N=N=N, and C≡C groups, which appear in both the ethanolic extract and AgNPs at 3381.5 cm-1 and 3434.6 cm-1, respectively. The ethanolic extract and AgNPs exhibit absorption bands at 2975.6 cm-1 and 2923.5 cm-1 respectively, in the presence of the C-H group. The ethanolic extract exhibits absorption bands at 1652.7 cm^{-1}, while AgNPs exhibits absorption bands at 1633.4 cm^{-1} in the presence of N=N=N and C≡C groups, respectively.

For roselle, as shown in figure (7), the absorption bands appear in the exanolic extract only in the presence of N=N=N, C≡C, Amide and C-O groups at 1401, 1226.5, 1048.1, 874.5and 428.1 cm^{-1}. While, they appear in both, the ethanolic extract and AgNPs in the presence of O-H and C-H groups at 3441.3, 2923.5, 1637.3 and 513.9 cm^{-1}.

According to figure (8), the green tea extract absorption bands appear in the ethanolic extract only in the presence of C-O, C-C, COO, amide, and C-H groups. However, they appear in both ethanolic extract and AgNPs in the presence of O-H, C-H, N=N=N, C≡C, C=O, and C-O groups.

Table (5) shows that outcomes are more likely to be related to flavonoids, which may be responsible for reduced AgNPs and their stability. These similar to the study conducted of Abbasi et al. (2017), who noted that AgNPs functionalized with biomolecules from the plant's aqueous extract acted as capping agents and stabilise the nanoparticles, according to FTIR spectroscopy. Along with some small changes in peak location, they observed that the similarities in results between extracts and its AgNPs clearly suggest the presence of residual plant extract in the samples acting as an AgNPs capping agent.

X-ray diffraction (XRD) of ginger AgNPs

It is well known that using ginger in various culinary and medical applications has several health benefits. According to our study, ginger is one of the most promising plants because it has a high antioxidant content.

The zeta potential data of the biosynthesized AgNP of ginger ethanolic extract, revealed that the zeta potential recorded -31.06 mV (phase shift: 53 rad/s, cell current: -31.06 mA, mobility: -2.31, run time: 0:05:02). It is widely known that the value of the zeta potential expresses the stability of the generated NPs. According to Nimesh et al. (2017), AgNP from ginger has moderate stability, as it ranges between ±30 to ±40 mV due to electrostatic repulsion. In general, the suspension with an absolute zeta potential less than 20 mV is unstable and will result in particle precipitation from solution, whereas a suspension with an absolute zeta potential greater than 20 mV is stable, which indicates the stability of ginger AgNP suspension. Further, Youssif et al. (2020) mentioned that the high level of zeta potential validates the high electrical charge on the nanoparticle surface that creates a strong repulsive force within and between nanoparticles to restrict agglomeration.

Cytotoxic activity of ginger AgNp against HepG2

The cytotoxicity of ginger AgNP on a human liver cell line (HepG2) in comparison to doxorubicin as a standard is one of the aims of this investigation. The results of liver cancer cell lines

(HepG2) after treatment with different concentrations of ginger AgNP are shown in Table (6) and Figure (12). The results indicate that HepG2 has a good resistance against ginger NP, with an IC50 of 424.62± 15.23 µg/mL, while Dox has a higher cytotoxicity effect with an IC50 of 92.05 µg/mL. The cytotoxic activity increased with the increase in treatment concentration from 31.25 to 1000 µg/mL. So, the highest concentration of 1000 µg/mL possesses the highest cytotoxic activity with both ginger AgNp and Dox. At a concentration of 1000 µg/mL, ginger AgNP has the same effect as DOX (97.30 and 97.39, respectively). Silver nanoparticles in tumour cells cause cytotoxicity by releasing Ag+ ions. NPs help in the production of reactive oxygen species and superoxide in mitochondria after oxygen is reduced by an electron from the electron transport chain. Excessive ROS induce oxidative damage to DNA, proteins, and lipids in cells, which ultimately results in cell death. When NPs are used to treat cancer cells, the nucleus may break down and fragment, destroying the cancer cell (Shalaby et al., 2022). In the liver cancer cell line HepG2, ginger extract may have an anticancer effect by eliminating superoxide radicals and hydrogen peroxide while replacing the functions of SOD, GPx, and CAT. Ginger contains a variety of biologically active chemicals, some of which have been identified by Tao et al. (2009) as 6-gingerol, 8-gingerol, and 10-gingerol. These active substances control several signal transduction pathways involved in the proliferation, angiogenesis, and metastasis of cancer cells. For example, 6-shogaol activated ROS and induced apoptosis in the cancer cell lines Huh-7 and HepG2 (Armentano et al., 2015). Additionally, the cytotoxicity increased with the concentration of synthesised NPs, suggesting their potential as an alternative therapeutic agent. Moreover, NPs are known to promote nucleic acid (DNA) repair in cells, inhibiting the development of tumour cells. However, NPs' surface-bound active components and antioxidants from plant extracts work as a preventative measure against oxidative stress-related disorders like tumours and inflammation (Pawar and Prabhu, 2019).

Table 6. Cytotoxic Activity of ginger AgNP and Dox against HepG2 cell line

Treatment	Conc. (µg/mL)	Viability %	Toxicity %	IC_{50} ± SD
Ginger AgNP	1000	2.70	97.30	424.62±5.92
	500	36.2	63.8	
	250	86.8	13.20	
	125	99.4	0.60	
	62.5	98.5	1.50	
	31.25	99.00	10	
Doxorubicin	1000	2.61	97.39	92.05±3.86
	500	3.28	96.72	
	250	11.57	88.43	
	125	24.58	75.42	
	62.5	73.68	26.32	
	31.25	95.34	4.66	

Values are mean ± SE. The IC_{50} values were determined from dose-effect curves by linear regression.

Conclusion

According to the findings of the current study, green chemistry has a significant impact on a variety of fields, including the health field, where we found that nanoparticles made from plants are very antioxidant-rich and exhibit potent anti-cancer and antioxidant activity. Plant-derived nanoparticles are extremely safe for both people and the environment. Many plants, including ginger, fenugreek, roselle,

red tea, and green tea, can be used to create green nanoparticles since they contain a variety of active compounds, such as phenolics, flavonoids, and catechins. According to the study's findings, ginger is a promising plant that can be applied as a preventive green nanoparticle, as it has many benefits and has a cytotoxic effect on HepG2 cells. Although our research has focused on the therapeutic applications of AgNPs, additional studies in animal models are required to establish the mechanisms and develop a complete understanding of the bioactivity and toxicity of AgNPs.

Availability of data and materials:

They are available as Supporting information.

Ethics approval and consent to participate:

Not applicable in this section.

Consent for publication:

All authors read and approved the final manuscript.

Conflicts of Interest:

The authors declare no conflict of interest.

Funding

Not applicable

REFERENCES

Abbasi, Z. Feizi, S., Taghipour, E. and Ghadam, P. (2017). Green synthesis of silver nanoparticles using aqueous extract of dried Juglans regia green husk and examination of its biological properties. Green Process Synth., 6: 477–485.

Ahmed, KK.M. and Baral, M. (2011).Tea polyphenols as antioxidants. Free Radicals and Antioxidants, 1(2): 02-03.

Armentano, M.F., Bisaccia, F., Miglionico, R., Russo, D., Nolfi, N., Carmosino, M., Andrade, P.B. Valentao, P., Sissokho, D. and Milella, L. (2015). Antioxidant and proapototic activities of Sclerocarya birrea [(A. Rich.) Hochst] methanolic root extract on the hepatocellular carcinoma cell line HegG2. Anticancer Properties of Natural Products, 2015: 1-11.

Belyagoubi-benhammou, N., Belyagoubi, L. and Bekkara, F.A. (2014). Phenolic contents and antioxidant activities in vitro of some selected Algerian plants. J. Med. Plants Res., 8 (40):1198-1207.

Dhillon, B., Awasthi, T., Sodhi, N.S., Sogi, D.S. and Jaiswal, S. (2021). A comparative study to investigate the effects of addition of milk and sugar on total polyphenol, flavonoid, catechin and tannin contents of green and black teas consumed in India. Journal of Food Measurement and Characterization,15(5): 4652-4658.

Chandran, S.P., Chaudhary, M., Pasricha, R., Ahmad, A. and Sastry, M. (2006). Synthesis of gold nanotriangles and silver nanoparticles using Aloe vera plant extract. Biotechnol. Prog., 22:577–583.

Chang, C.-C., Yang, M.-H., Wen, H.-M. and Chern, J.-C. (2002). Estimation of total flavonoid content in propolis by two complementary colometric methods. Journal of Food and Drug Analysis, 10(3): 178-182.

Dwivedi, A., and Gopal, K. (2010).Biosynthesis of silver and gold nanoparticles using Chenopodium album leaf extract. Colloids Surf. A Physicochem. Eng. Asp. 369, 27–33.

Firoozi, S., Jamzad, M. and Yari, M. (2016). Biologically synthesized silver nanoparticles by aqueous extract of Satureja intermedia C.A. Mey and the evaluation of total phenolic and flavonoid contents and antioxidant activity. J. Nanostruct. Chem., 6: 357–364.

Gaber, N.B., El-Dahy, S.I. and Shalaby, E.A. (2021). Comparison of ABTS, DPPH, permanganate, and methylene blue assays for determining antioxidant potential of successive extracts from pomegranate and guava residues. Biomass Conversion and Biorefinery, 1-10.

Ghasemzadeh, A., Jaafar, H.Z. and Rahmat, A. (2010). Antioxidant activities, total phenolics and flavonoids content in two varieties of Malaysia young ginger (Zingiber officinale Roscoe). Molecules, 15(6): 4324-4333.

Gopinath, K., Gowri, S., Karthika, V. and Arumugam, A. (2014). Green synthesis of gold nanoparticles from fruit extract of Terminalia arjuna, for the enhanced seed germination activity of Gloriosa superba. Journal of Nanostructure in Chemistry, 4: 115.

Hano, C. and Abbasi, B.H. (2022). Plant-Based Green Synthesis of Nanoparticles: Production, Characterization and Applications. Biomolecules, 12(1): 31.

Huang, J., Li, Q., Sun, D., Lu, Y., Su, Y., Yang, X., Wanh, H., Wang, Y., Shao, W., He, N., Hong, J. and Chen C. (2007).Biosynthesis of silver and gold nanoparticles by novel sun dried Cinnamomum canphora leaf, Nanotech., 18, 1–11. Iravani, S. (2011). Critical review – green synthesis of metal nanoparticles using plants. Green Chem., 13:2638–2650.

Jeevanandam, J., Barhoum, A., Chan, Y.S., Dufresne, A. and Danquah, M.K. (2018). Review on nanoparticles and nanostructured materials: history, sources, toxicity and regulations. Beilstein J Nanotechnol. 9: 1050–1074.

Khattak, U., Ullah, R., Khan, S., Afriq, S., Rauf, A. and Hassanien M. (2019).Synthesis, characteristics and biological activities of silver nanoparticles from Euphorbia dracunculoides, Eur Asia J. BioSci. 13 (2): 2249–2260.

Kokila, N.R., Mahesha, B., Roopab, K.P,. Daruka Prasadc, B., Kalyan Rajd, S.N. Manjulae, K. and Mruthunjayaf, R. R.. (2022).Thunbergia mysorensis mediated nano silver oxide for enhanced antibacterial, antioxidant, anticancer potential and in vitro hemolysis evaluation. J. Mol. Struct., 1255: 13245.

Lee, H-J., Lee, G., Jang, N.R. Yun, J.H., Song, J.Y. and Kim, B.S. (2011). Biological synthesis of copper nanoparticles using plant extract. Nanotechnology 1:371–374

Li, X., Xu, H., Chen, Z.S. and Chen, G. (2011). Biosynthesis of nanoparticles by microorganisms and their applications. J Nanomater, 8: 1–16.

Liu, X., Chen, J-L., Yang, W-Y., Qian, Y-C., Pan, J-Y., Zhu, C-N., Liu, L., Ou, W-B., Zhao, H-X. and Zhang, D-P. (2021). Biosynthesis of silver nanoparticles with antimicrobial and anticancer properties using two novel yeasts. Scientific Reports, 11: 15795.

Mittal A.K., Chisti Y. and Banerjee U.C. (2013). Synthesis of metallic nanoparticles using plant extracts. Biotechnol. Adv., 31:346–356.

Nimesh, S., Chandra, R. and Gupta N. (2017). Methods or characterization of nanoparticles, Advances in Nanomedicine for the Delivery of Therapeutic Nucleic Acids, p. 43–58.

Pawar, A. and Prabhu, P. (2019). Nanosoldiers: a promising strategy to combat triple neg- ative breast cancer, Biomed. Pharmacother. 110 319–341.

Ramesh, A.V., Devi, D.R., Battu, G. and Basavaiah, K. (2018). A facile plant mediated synthesis of silver nanoparticles using an aqueous leaf extract of Ficus hispida Linn. F. for catalytic. antioxidant and antibacterial applications. S. Afr. J. Chem. Eng., 26: 24–34.

Re, R., Pellegrini, N., Proteggente, A., Pannala, A., Yang, M. and Rice-Evans, C. (1999). Antioxidant activity applying an improved ABTS radical cation decolorization assay. Free Radic. Biol. Med. 26, 1231-1237.

Rossenthaler, L. (1930). The chemical investigation of plants. Translated into English by Sudhamoy Ghosh from the Third German edition. Bell and Sons. Ltd London.

Shalaby, E. A., Shanab, S.M.M., Abd El-Raheem, W.M. and Hanafy, E.A. (2022). Biological activities and antioxidant potential of different biosynthesized nanoparticles of Moringa oleifera. Scientific Reports, 12:1-14.

Singh, R., Nawale, L.U., Arkile, M., Shedbalkar, U.U., Wadhwani, S.A., Sakar, D. and Chopade, B.A. (2015). Chemical and biological metal nanoparticles as antimycobacterial agents: A comparative study. Int J Antimicrob Agents 46(2): 183-188.

Sintubin, L., De Windt, W., Dick, J., Mast, J., Van Der Ha, D., Verstraete, W. and Boon, N. (2009). Lactic acid bacteria as reducing and capping agent for the fast and efficient production of silver nanoparticles. Appl. Microbiol. Biotechnol. 84, 741–749.

Slater, T., Sawyer, B. and Straeuli, U. (1963). Studies on succinate-tetrazolium reductase systems. III. Points of coupling of four different tetrazolium salts. Biochem. Biophys. Acta 77:383.

Swain, T. and Hillis, W.E. (1959).The Phenolic Constituents of Prunus domestica. I.—The Quantitative Analysis of Phenolic Constituents. Journal of the Science of Food and Agriculture, 10, 63-68.

Tak, Y.K., Pal, S.; Naoghare, P.K., Rangasamy, S. and Song, J.M. (2015). Shape-Dependent Skin Penetration of Silver Nanoparticles: Does It Really Matter? Sci. Rep., 5: 16908.

Tang, G.Y., Zhao, C.N., Xu, X.Y., Gan, R.Y. Cao, S.Y., Liu, Q., Shang, A., Mao, Q.Q, and Li, H.B. (2019). Phytochemical composition and antioxidant capacity of 30 Chinese teas. Antioxidants (Basel), 8(6):180.

Tao, Y., Li, W., Liang, W. and Breemen, R.B. (2009).Identification and quantification of gingerols and related compounds in ginger dietary supplements using high-performance liquid chromatography-tandem mass spectrometry. Journal of Agricultural and Food Chemistry, 57(21):10014-10021.

Wang, C.Y., Chen, Y.W. and Hou, C.Y. (2019). Antioxidant and antibacterial activity of seven predominant terpenoids. International Journal of food properties, 22(1): 230-238.

Yazdanian, M., Rostamzadeh, P., Rahbar, M., Alam, M., Abbasi, K., Tahmasebi, E., Tebyaniyan, H., Ranjbar, R., Seifalian, A. and Yazdanian, A. (2022).The Potential Application of Green-Synthesized Metal Nanoparticles in Dentistry: A Comprehensive Review. Bioinorg Chem Appl. 2022: 2311910.

Yen, G.C., Chen, H.Y. (1995). Antioxidant activity of various tea extracts in relation to their antimutagenecity. J Agri Food Chem. 43: 27–37.

Youssif, K.A., Elshamy, A.M., Rabeh, M.A., Gabr, N., Afifi, W.M., Salem, M.A., Albohy, A., Abdelmohsen, U.R. and Haggag, E.G. (2020).Cytotoxic Potential of Green Synthesized Silver Nanoparticles of Lampranthus coccineus Extracts, Metabolic Profiling and Molecular Docking Study. ChemistrySelect, 5(39): 12278-12286.